

Forkhead Box M1 Regulates Quiescence-Associated Radioresistance of Human Head and Neck Squamous Carcinoma Cells

Jaimee C. Eckers,^a Amanda L. Kalen,^a Ehab H. Sarsour,^a Van S. Tompkins,^b Siegfried Janz,^b Jyung Mean Son,^a Claire M. Doskey,^a Garry R. Buettner^a and Prabhat C. Goswami^{a,1}

^a Free Radical and Radiation Biology Division, Department of Radiation Oncology, and ^b Department of Pathology, University of Iowa, Iowa City, Iowa

Eckers, J. C., Kalen, A. L., Sarsour, E. H., Tompkins, V. S., Janz, S., Son, J. M., Doskey, C. M., Buettner, G. R. and Goswami, P. C. Forkhead Box M1 Regulates Quiescence-Associated Radioresistance of Human Head and Neck Squamous Carcinoma Cells. *Radiat. Res.* 182, 420–429 (2014).

Cellular quiescence is a reversible growth arrest in which cells retain their ability to enter into and exit from the proliferative cycle. This study investigates the hypothesis that cell growth-state specific oxidative stress response regulates radiosensitivity of cancer cells. Results showed that quiescent (low proliferative index; >75% G₀ phase and lower RNA content) Cal27 and FaDu human head and neck squamous cell carcinoma (HNSCC) are radioresistant compared to proliferating cells. Quiescent cells exhibited a three to tenfold increase in mRNA levels of Mn-superoxide dismutase (MnSOD), dual oxidase 2 (DUOX2) and dual-specificity phosphatase 1 (DUSP1), while mRNA levels of catalase (CAT), peroxiredoxin 3 (PRDX3) and C-C motif ligand 5 (CCL5) were approximately two to threefold lower compared to proliferating cells. mRNA levels of forkhead box M1 (FOXM1) showed the largest decrease in quiescent cells at approximately 18-fold. Surprisingly, radiation treatment resulted in a distinct gene expression pattern that is specific to proliferating and quiescent cells. Specifically, FOXM1 expression increased two to threefold in irradiated quiescent cells, while the same treatment had no net effect on FOXM1 mRNA expression in proliferating cells. RNA interference and pharmacological-based downregulation of FOXM1 abrogated radioresistance of quiescent cells. Furthermore, radioresistance of quiescent cells was associated with an increase in glucose consumption and expression of glucose-6-phosphate dehydrogenase (G6PD). Knockdown of FOXM1 resulted in a significant decrease in G6PD expression, and pharmacological-inhibition of G6PD sensitized quiescent cells to radiation. Taken together, these results suggest that targeting FOXM1 may overcome radioresistance of quiescent HNSCC. © 2014 by Radiation Research Society

INTRODUCTION

Human solid tumors are believed to consist of three different cell populations: rapidly proliferating or cycling population, quiescent or non-cycling population and irreversible growth-arrested population. Cellular quiescence (G₀) is a reversible growth arrest in which cells retain their capacity to re-enter the proliferative cycle (G₁, S, G₂ and M phases). Although quiescent cells are not actively proliferating, they are metabolically active (1, 2). Quiescent cancer cells are resistant to therapies that are designed to kill proliferating cancer cells (i.e., chemotherapy and radiation therapy) (3, 4). Thus, quiescent cancer cells are believed to be a primary reason for tumor recurrence.

Radiation therapy alone or more often in combination with chemotherapy is used as a standard of care for locally advanced human head and neck squamous cell carcinoma (HNSCC) (5). Radiation is well known to generate reactive oxygen species (ROS) that cause oxidative damage to cellular macromolecules that can result in toxicity. Therefore, cellular antioxidant status is believed to have a critical role in regulating radiation response (6–9). The cellular antioxidant network includes small molecular weight antioxidants (vitamin C, glutathione, thioredoxin and glutaredoxins) and antioxidant enzymes (superoxide dismutases, glutathione peroxidases, catalase and the six-member family of peroxiredoxins). Although the mechanisms regulating quiescence-associated radioresistance are not well understood, it is believed that the distinct difference in the redox environment between quiescent and proliferating cells may have a regulatory role in cell growth-state specific radiation response (10, 11). We and others have shown that the activity of manganese superoxide dismutase (MnSOD) is maximal in quiescent (G₀) cells and its activity decreases as cells progress through the cell cycle coinciding with a shift in the cellular redox status towards a more oxidizing environment (12–14). An oxidizing environment may sensitize proliferating cells more towards radiation-induced toxicity compared to quiescent cells that have a higher antioxidant capacity.

A less well known oxidative stress response gene that is differentially expressed in proliferating and quiescent cells

Editor's note. The online version of this article (DOI: 10.1667/RR13726.1) contains supplementary information that is available to all authorized users.

¹ Address for correspondence: Free Radical and Radiation Biology Division, Department of Radiation Oncology, University of Iowa, Iowa City, IA 52242-1181; e-mail: prabhat-goswami@uiowa.edu.

is forkhead box M1 (FOXMI), which belongs to the forkhead box (FOX) family of transcription factors known to play important roles in regulation of gene expression involved in cell growth, proliferation, differentiation and aging (15, 16). All Fox proteins possess a winged helix DNA binding motif containing a sequence of 80–100 amino acids (17). FOXMI is preferentially expressed in proliferating cells (18–21). FOXMI expression peaks in the G₂ phase (18) and is overexpressed in most malignancies, including all carcinomas (22). Additionally, FOXMI has been shown to regulate several well known antioxidant genes such as MnSOD, catalase (CAT) and peroxiredoxin 3 (PRDX3) (23), suggesting that FOXMI could regulate the cellular redox environment and radiation response.

Results from our current study now show that quiescent HNSCCs are radioresistant compared to proliferating cells. Additionally, although basal expression of FOXMI is much lower in quiescent cells than proliferating cells, there is a fourfold increase in FOXMI in irradiated quiescent cancer cells that is not observed in irradiated proliferating cancer cells. Furthermore, both pharmacological (thiostrepton) and RNA interference (RNAi)-mediated knockdown of FOXMI resulted in quiescent HNSCC becoming more sensitive to radiation. Knockdown of FOXMI also resulted in the downregulation of glucose-6-phosphate dehydrogenase expression, a rate limiting step of the pentose phosphate pathway. These results suggest FOXMI regulates radioresistance of quiescent HNSCC possibly by activating the pentose phosphate pathway.

MATERIALS AND METHODS

Cell Culture

Human squamous cell carcinoma cell lines of tongue (Cal27; CRL-2095) and pharynx (FaDu; HTB-43) origin were obtained from the American Type Culture Collection (ATCC®, Manassas, VA) and cultured in high glucose Dulbecco's modified Eagle's medium (DMEM) supplemented with 10% fetal bovine serum (FBS) and antibiotics. Cells plated at low density (1 million cells/100 mm culture dish) and grown for 24 h prior to irradiation were considered to be proliferating. Cells cultured for at least 7 days with the media changed every 3 days were considered to be in a quiescent state. Flow cytometry assays were used to assess quiescence. Ethanol-fixed Cal27 cells representative of low and high proliferative index were incubated with Hoechst 33258 (for DNA) and Pyronin Y (for RNA), and fluorescence analyzed by Aria™ II flow cytometer: Hoechst 33258, excitation at 355 nm and emission at 400 nm band pass filter; Pyronin Y, excitation at 561 nm and emission at 570–600 nm band pass filter. Flow cytometry measurements of Hoechst 33258 fluorescence (DNA content) were used to assess cell cycle phase distributions. For this study, cultures with a lower proliferative index (S phase <10%; G₁ phase >75%; lower RNA content) were considered to be in a quiescent state and cultures with a higher proliferative index (S phase >30%; G₁ phase <40%; higher RNA content) were considered to be in a proliferative state.

Irradiations were performed using a cesium-137 gamma radiation source (dose rate: 0.71 Gy/min). Cell survival was measured using a clonogenic assay and flow cytometry measurements of propidium iodide dye exclusion following our previously published protocols (24). Thiostrepton (TS) and dehydroepiandrosterone (DHEA) were

purchased from Sigma-Aldrich® (St. Louis, MO). To measure glucose consumption, cultures were incubated for 4–6 h with DMEM and glucose concentration was measured using a Bayer Glucometer Elite® with Bayer Ascensia Elite Blood glucose test strips (12, 25). Glucose consumption rate was calculated per cell per hour.

Human Antioxidant Mechanisms Array

Total cellular RNA was reverse transcribed using High Capacity cDNA Reverse Transcription Kit (Applied Biosystems®). cDNA was used in the TaqMan® Human Antioxidant Mechanism Array (Applied Biosystems), which was run on an Applied Biosystems StepOne Plus® machine. Results were analyzed using the StepOne Plus and DataAssist® software v3.0 (Applied Biosystems) following our previously published protocol (24).

Quantitative Real Time Polymerase Chain Reaction (PCR)

Power SYBR Green and the StepOnePlus™ System (Applied Biosystems) were used for the quantitative Real Time PCR (Q-PCR) assay. Primer sequences for individual genes used in the Q-PCR assay are shown in Supplementary Table S1 (<http://dx.doi.org/10.1667/RR13726.1.S1>). The cycle threshold (C_T) was determined from the linear range of amplification and normalized to 18S rRNA levels for individual samples. The relative mRNA levels were calculated as follows: ΔC_T (sample) = C_T (mRNA of interest) – C_T (18S); $\Delta \Delta C_T$ = ΔC_T (post-treatment time point) – ΔC_T (control); relative expression = $2^{-\Delta \Delta C_T}$. Fold change in individual mRNA levels was calculated relative to corresponding mRNA levels in control cells (24).

Immunoblotting

Cellular monolayers were collected in radioimmunoprecipitation assay buffer supplemented with PhosSTOP (Roche Diagnostics, Indianapolis, IN) and protease (Thermo Scientific, Waltham, MA) inhibitors. Equal amounts of proteins were separated by sodium dodecyl sulfate polyacrylamide gel electrophoresis and proteins were transferred to a nitrocellulose membrane. Blots were incubated with primary antibodies to FOXMI (1:200; Santa Cruz Biotechnology Inc., Dallas, TX) and glucose-6-phosphate dehydrogenase (G6PD) (1:1,000; Bethyl Laboratories Inc., Montgomery, TX). Immunoreactive polypeptide was visualized using ECL Plus reagent and Typhoon 7000 Phosphorimager (GE Healthcare Bio-Sciences, Pittsburgh, PA). Blots were reprobbed with antibodies to actin (1:3,000; Santa Cruz Biotechnology Inc.) and fold change calculated using ImageJ software.

Flow Cytometry Assays

Analysis of cell viability. Flow cytometry measurements of cell viability were assessed by measuring propidium iodide (PI) dye exclusion. Cells resuspended in cold phosphate buffered saline were incubated with PI (1 µg/mL) and fluorescence from 10,000 cells was collected in list mode. The percentages of PI-positive (nonviable) and negative (viable) cells were calculated using WinMDI software (Scripps Research Institute®, La Jolla, CA).

Analysis of cell cycle phases. Ethanol-fixed cells were treated with RNase A (0.1 mg/ml) for 30 min, followed by incubation with PI dye (35 µg/ml). DNA content of PI-stained cells was analyzed by FACScan™ (Becton, Dickinson Co., Franklin Lakes, NJ) and the percentage of cells in G₁, S, G₂ and M phases was calculated using ModFit software (Verity Software House, Topsham, ME) following our previously published protocol (6).

Generation of inducible FOXMI-knockdown cell lines. TRIPZ FOXMI shRNA vector targeting FOXMI and control TRIPZ vector containing a nonmammalian targeting shRNA sequence were purchased from Open Biosystems (Thermo Scientific). Lentiviruses were generated using the Trans-Lentiviral Packaging Kit (Thermo

Fisher Scientific Inc., Waltham, MA). 293T cells (TSA201 subclone) were transfected using calcium phosphate precipitation with the TRIPZ vector and helper plasmid cocktail following the manufacturer's protocol. Viral supernatant was used to infect cells. Puromycin (1 $\mu\text{g/ml}$) resistant cells were further incubated with doxycycline (1 $\mu\text{g/ml}$) to induce FOXM1 shRNA expression. Red fluorescent protein (RFP) positive cells, Q-PCR and Western blotting were used to verify FOXM1 shRNA expression.

Statistical Analysis

Statistical analysis was done using the one- and two-way analysis of variance with LSD significant difference test; the Student's *t* test was used for experiments with less than three groups. Homogeneity of variance was assumed with 95% confidence interval level. Results from at least three independent experiments with $P < 0.05$ were considered significant. All statistical analyses were done using SPSS version 17 and Microsoft Excel.

RESULTS

Quiescent Head and Neck Cancer Cells Are Resistant to Ionizing Radiation Treatment Compared to Proliferating Cells

It is believed that cancer cell growth state plays a significant role in therapy response. To determine if cell growth state influences radiation response of human oral squamous cancer cells, we optimized cell culture conditions that are representative of quiescent (low proliferative index) and proliferating (high proliferative index) states. Cal27 cells were cultured to obtain monolayers with low and high cell density. Monolayer cultures were trypsinized and ethanol-fixed cells were analyzed for RNA and DNA content using flow cytometry. Our results show that cultures with a higher cell density had a lower RNA content compared with RNA content of cultures with a lower cell density (Fig. 1A). Cultures with a lower RNA content had less than 10% S-phase cells and more than 75% G₁-phase cells (Fig. 1B). Cultures with a higher RNA content were associated with more than 30% S-phase cells and less than 40% G₁-phase cells (Fig. 1B). For this study, we considered cultures with a lower RNA content and more than 75% G₁-phase cells as quiescent cultures (lower proliferative index), and cultures with a higher RNA content and less than 40% G₁-phase cells were considered as proliferating cultures (higher proliferative index).

HNSCC (Cal27 and FaDu) with low and high proliferative indices were irradiated with 2 and 4 Gy, and a clonogenic assay was used to assess cell survival. A dose-dependent toxicity was observed for both growth states in the two cell lines [Fig. 1C (Supplementary Fig. S1; <http://dx.doi.org/10.1667/RR13726.1.S1>)]. Cal27 cultures with a higher proliferative index showed a surviving fraction of 0.45 and 0.2 in 2 and 4 Gy irradiated cells, respectively, while Cal27 cells with a lower proliferative index had a surviving fraction of 0.8 and 0.65 (Fig. 1C). Comparable results were obtained in a separate HNSCC cell line [(FaDu cells) Supplementary Fig. S1; <http://dx.doi.org/10.1667/>

[RR13726.1.S1](http://dx.doi.org/10.1667/RR13726.1.S1)]. These results showed that cell growth states significantly impact radiation response of HNSCC.

Radiation Enhances FOXM1 Expression Selectively in Quiescent Cancer Cells

To determine if the cell growth state elicits a differential oxidative stress response after the radiation treatment, we first determined whether the basal mRNA levels of oxidative stress response genes differ in Cal27 cultures representative of low (quiescence) and high proliferative (proliferation) index. Total cellular RNA isolated from Cal27 quiescent and proliferating cultures was reverse transcribed and used in the TaqMan Human Antioxidant Mechanisms Array (Applied Biosystems) that includes 92 of the most commonly studied oxidative stress response genes. Whereas mRNA levels in the majority of the oxidative stress response genes were similar in proliferating and quiescent Cal27 cells, cell growth state related changes in the mRNA levels of a subset of these genes were observed (array data not shown). These results were further verified by performing a Q-RT-PCR assay (Fig. 1D). mRNA levels of catalase (CAT), peroxiredoxin 3 (PRDX3) and C-C motif ligand 5 (CCL5) were approximately two to threefold lower in quiescent cells, while mRNA levels of Mn-superoxide dismutase (MnSOD) and dual oxidase 2 (DUOX2) increased approximately tenfold, and mRNA levels of dual-specificity phosphatase 1 (DUSP1) showed approximately a threefold increase. mRNA levels of FOXM1 showed the largest decrease in quiescent cells, approximately 18-fold. The significant decrease in FOXM1 mRNA levels was also observed in quiescent FaDu cells (Supplementary Fig. S2A; <http://dx.doi.org/10.1667/RR13726.1.S1>). Quiescence related decreases in FOXM1 mRNA levels were also associated with decreases in its protein levels (Supplementary Fig. S2B; <http://dx.doi.org/10.1667/RR13726.1.S1>). These results showed that proliferating and quiescent HNSCC cells are characterized by distinct expression of specific oxidative stress response genes, suggesting that these genes could play a role in the cell growth-state specific radiation response.

To determine if radiation perturbs expression of the subset of oxidative stress response genes that were found to have a differential expression in quiescent compared to proliferating Cal27 cells (Fig. 1D), a q-RT-PCR assay was used to measure mRNA levels of these genes in control and 8 Gy irradiated proliferating and quiescent Cal27 cells. Indeed, irradiated cells showed a distinct gene expression pattern that is specific to proliferating and quiescent growth states. In irradiated proliferating cells, CCL5 and DUSP1 expression increased approximately six to tenfold, respectively (Fig. 2A), while the same treatment did not show any significant effect in CCL5 and DUSP1 mRNA levels in irradiated quiescent cells (Fig. 2B). An increase in CCL5 mRNA levels in irradiated proliferating cells could be an indication of an intracellular inflammatory response to

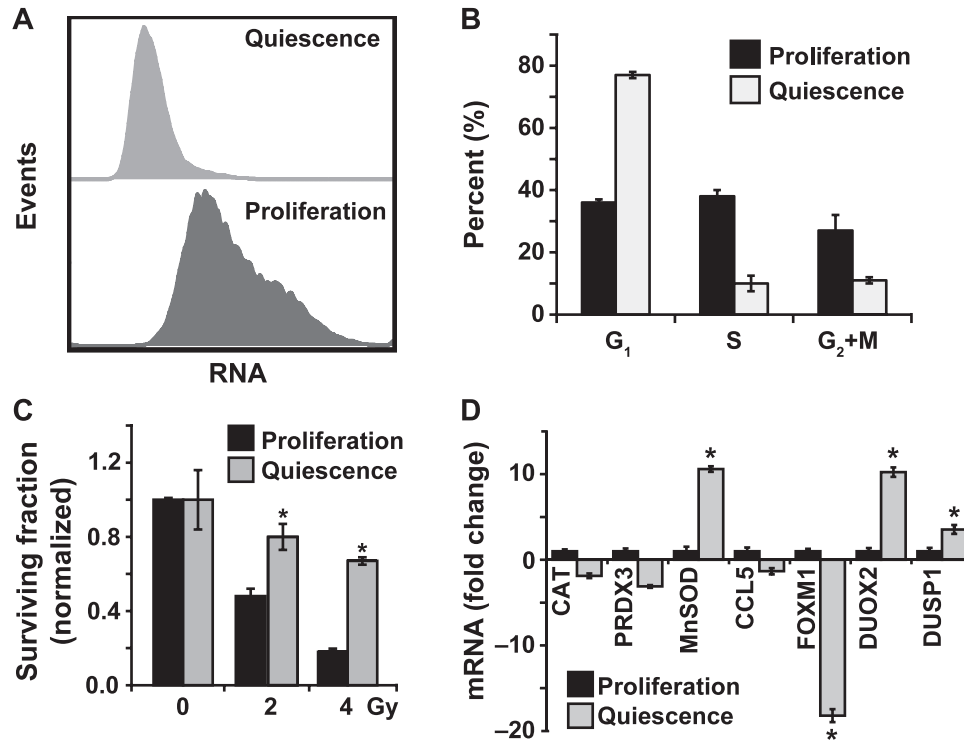


FIG. 1. Quiescent HNSCC are radioresistant and have lower basal FOXMI expression. Panel A: Flow cytometry assay to assess quiescence. Ethanol-fixed Cal27 cells representative of low and high proliferative index were incubated with Hoechst 33258 (for DNA) and Pyronin Y (for RNA), and fluorescence analyzed by Aria II flow cytometer. Panel B: Flow cytometry measurements of DNA content to examine cell cycle phase distributions. Cultures with a lower proliferative index (S phase <10%; G₁ phase >75%) are considered as quiescent and cultures with a higher proliferative index (S phase >30%; G₁ phase <40%) are considered as proliferating cells. Panel C: A clonogenic assay designed to accommodate post-lethal damage repair was used to examine surviving fraction in Cal27 cells. Panel D: A Q-RT-PCR assay was used to measure mRNA levels in proliferating and quiescent Cal27 cells. Fold change in mRNA levels in quiescent cells was calculated relative to corresponding mRNA levels in proliferating cells. Asterisks represent statistical significance of quiescent compared to proliferating cells. n = 3; $P < 0.05$.

irradiation, while the increase in DUSP1 mRNA levels could relate to radiation-induced activation of the cell cycle checkpoint pathways. In irradiated quiescent cells, there was a small but statistically significant increase in PRDX3 mRNA levels (approximately twofold) and decrease in DUOX2 (approximately twofold). Interestingly, FOXMI expression increased three to fourfold in irradiated quiescent cells, while its expression did not appear to change in irradiated proliferating cells (Fig. 2A and B). Because FOXMI is a transcription factor that has been recently reported to regulate expression of major antioxidant genes (23), we focused our efforts on whether FOXMI regulates radioresistance of quiescent cancer cells.

To determine if radiation induces a dose-dependent expression of FOXMI, q-RT-PCR and Western blotting assays were performed to measure FOXMI mRNA and protein levels in 0–8 Gy irradiated quiescent cultures of Cal27 and FaDu cells (Fig. 2C and D). FOXMI mRNA levels increased approximately 1.5- to 2-fold in 2 and 4 Gy irradiated Cal27 quiescent cultures and an increase of 2.5- to 3-fold was observed in 6 and 8 Gy irradiated cells (Fig. 2C). The dose-dependent increase in FOXMI mRNA levels was

also associated with a corresponding increase in its protein levels (Fig. 2C). A dose-dependent increase in FOXMI mRNA and protein was also reproduced in the independent cell line, FaDu (Fig. 2D). Because FOXMI expression is closely related to cell cycle progression through S, G₂ and M phases, flow cytometry was used to determine whether the increase in FOXMI expression was associated with re-entry into the cell cycle after irradiation. These results showed that the radiation-induced increases in FOXMI expression did not affect the cell cycle distribution of quiescent Cal27 cultures (Supplementary Fig. S3; <http://dx.doi.org/10.1667/RR13726.1.S1>). Taken together, these results suggest that FOXMI could function to regulate the response of quiescent cells to irradiation, independent of its ability to regulate the cell cycle.

Pharmacological and Molecular Inhibition of FOXMI Expression Exacerbates Radiation-Induced Toxicity in Quiescent Cal27 Cells

To determine whether FOXMI can regulate quiescence-associated radioresistance, FOXMI was inhibited using

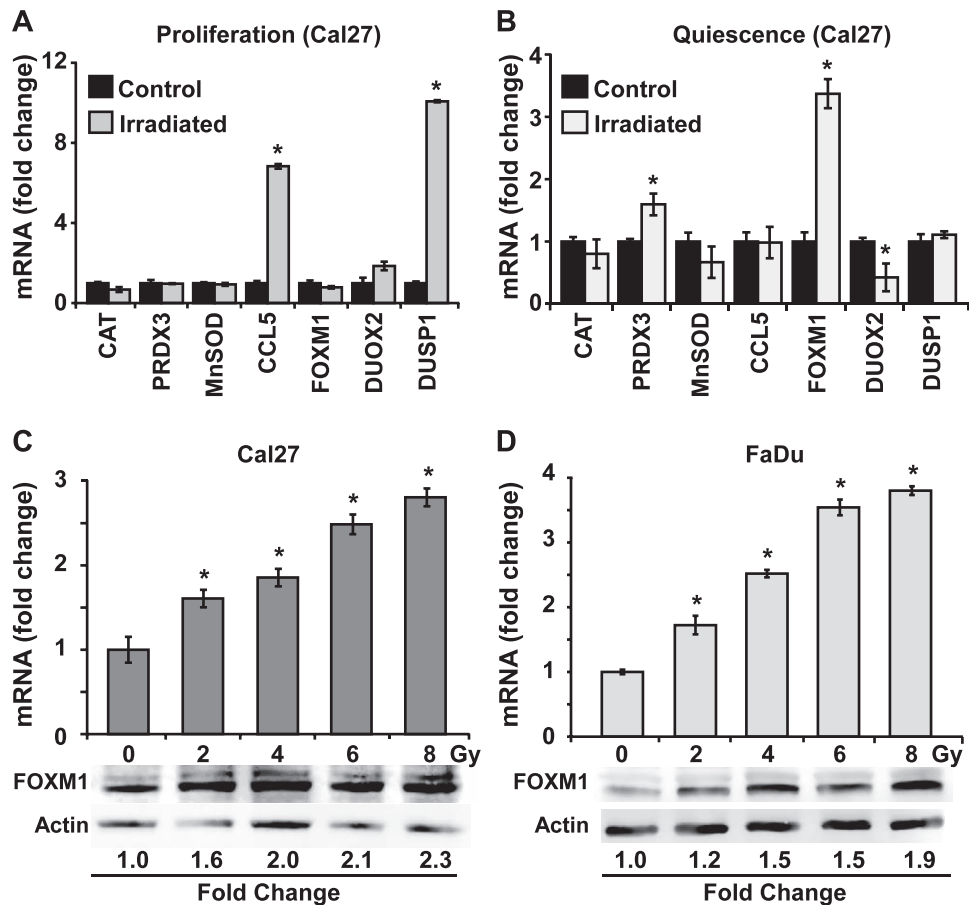


FIG. 2. Preferential induction of FOXM1 expression is associated with radioresistance of quiescent HNSCC. Q-RT-PCR measurements of expression of oxidative stress response genes in control and irradiated proliferating (panel A) and quiescent (panel B) Cal27 cells. Asterisks represent statistical significance compared to individual mRNAs in unirradiated cells. $n = 3$; $P < 0.05$. FOXM1 mRNA and protein levels in 0–8 Gy irradiated quiescent Cal27 (panel C) and FaDu (panel D) cells measured at 48 h postirradiation. Asterisks represent statistical significance compared to unirradiated cells. $n = 3$; $P < 0.05$.

thiostrepton (26–28). Thiostrepton is a natural cyclic oligopeptide thiazole antibiotic (26) whose inhibitory activity is largely due to its action as a proteasome inhibitor (27). Although the exact mechanisms regulating FOXM1 mRNA levels in thiostrepton-treated cells are unknown, it is possible that the thiostrepton-induced inhibition of the proteasome could stabilize mRNA-destabilizing proteins, which in turn downregulate FOXM1 mRNA levels (27). Quiescent Cal27 cultures were treated for 24 h with 0–10 μM thiostrepton and FOXM1 mRNA levels were measured using q-RT-PCR (Fig. 3A). Results showed a dose-dependent decrease in FOXM1 mRNA levels, approximately 50% decrease in cells treated with 1 μM thiostrepton and more than 90% decrease in 10 μM thiostrepton treated cells. Results from a clonogenic assay showed a dose-dependent toxicity of thiostrepton in Cal27 and FaDu quiescent cultures (Fig. 3B and C). Cell survival for either cell line was approximately 80% in 5 μM and 40% in 10 μM thiostrepton treated cells (Fig. 3B and C). For combination treatments, quiescent cultures were treated with 5 or 10 μM thiostrepton for 24 h and then 2 Gy irradiated. For both cell

lines, the combination of thiostrepton and irradiation significantly reduced survival compared to either treatment alone. These data suggest that pharmacologically reducing the level of FOXM1 sensitizes quiescent Cal27 and FaDu cells to radiation-mediated toxicity.

The causality of FOXM1 regulating radioresistance of quiescent HNSCC was further evaluated using a molecular genetic approach. Cal27 cells carrying a doxycycline-inducible FOXM1 shRNA were generated and tested for FOXM1 mRNA and protein levels (Fig. 4A). All three FOXM1 shRNA constructs decreased FOXM1 mRNA levels by more than 70%. Because FOXM1 mRNA and protein levels were significantly decreased in doxycycline treated Cal27 cells carrying the shFOXM1-2 construct, this cell line was further used for the measurements of radiation-induced toxicity. Cell survival was measured using both a clonogenic assay and flow cytometry for PI-dye exclusion. Representative dishes with colonies are shown in Fig. 4B and results are quantitated in Fig. 4C. As anticipated, radiation treatment alone showed a dose-dependent decrease in cell survival, with approximately 75% survival in 2 Gy

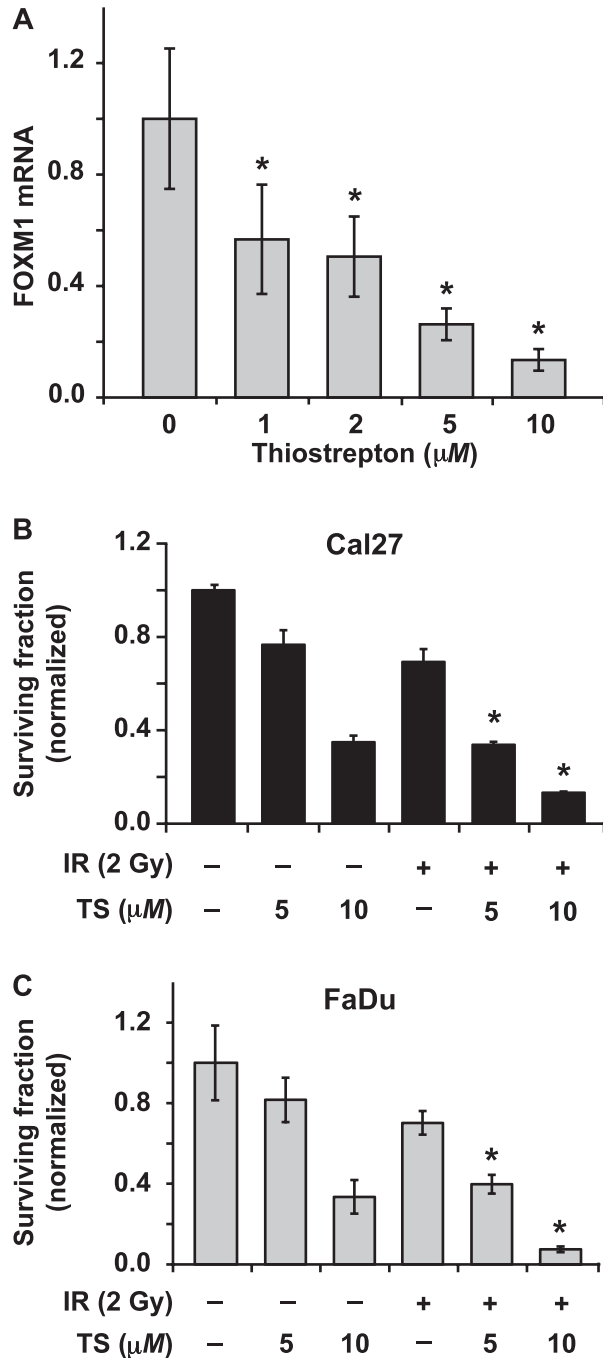


FIG. 3. Thiostrepton-induced downregulation of FOXM1 sensitizes quiescent HNSCC to radiation. Panel A: A Q-RT-PCR assay was used to measure FOXM1 mRNA expression in control and thiostrepton (0–10 μM) treated Cal27 cells. Asterisk represents statistical significance compared to untreated cells. $n = 3$; $P < 0.05$. A clonogenic assay was used to examine cell survival in irradiated Cal27 (panel B) and FaDu (panel C) cells pretreated with thiostrepton 24 h prior to irradiation. Asterisks represent statistical significance of combined treatment compared to radiation or thiostrepton treatment alone. $n = 3$; $P < 0.05$.

irradiated cells and 55% survival in 4 Gy irradiated cells (Fig. 4C). Notably, FOXM1 knockdown cells were more sensitive to radiation-induced cell killing, with approximately 35% survival in 2 Gy irradiated cells and 15%

survival in 4 Gy irradiated cells. FOXM1 was also shown to regulate survival of irradiated quiescent Cal27 cells, flow cytometry measurements of PI-dye exclusion (Fig. 4D). The percentage of PI-positive cells (indicative of nonviable cells) increased approximately 20, 40 and 50% in 2, 4 and 8 Gy irradiated cells, respectively, at 12 days postirradiation. Cells with reduced levels of FOXM1 and that were 2, 4 and 8 Gy irradiated showed approximately 50, 70 and 80% PI-positive cells, respectively. Overall, these results demonstrate that FOXM1 regulates radioresistance of quiescent Cal27 HNSCC.

FOXMI Regulated Radioresistance of Quiescent Cancer Cells is Mediated, in Part, Through Activation of the Pentose Phosphate Pathway

Oxidative stress is known to affect cellular metabolism by altering glucose metabolism (29, 30). Previous studies report that the pentose phosphate pathway influences radiosensitivity (31, 32). Because it is well known that radiation induces oxidative stress, experiments were performed to measure glucose consumption in control and irradiated quiescent Cal27 cells following our previously published method (12, 25). Our data show that radiation treatment increased the glucose consumption rate from 1.0 ± 0.07 pmole cell⁻¹ h⁻¹ in control unirradiated cells to 1.77 ± 0.24 pmole cell⁻¹ h⁻¹ in irradiated cells (Fig. 5A). Results from a q-RT-PCR assay showed approximately a twofold increase in G6PD mRNA levels (Fig. 5B). G6PD catalyzes the rate limiting step in the pentose phosphate pathway.

We then asked whether G6PD could be a transcriptional target of FOXM1, first by employing a bioinformatics approach. Indeed, the FOXM1 target sequence, “TGT TTTGTT”, was identified in the second intron of G6PD (+140; NG_009015). shRNA mediated knock-down of FOXM1 expression was associated with a significant decrease in G6PD mRNA and protein levels (Fig. 5C). These results suggest that G6PD could be a transcriptional target of FOXM1 in quiescent Cal27 cells. To determine the causality of G6PD regulating radiation response of Cal27 cells, quiescent Cal27 cultures were incubated with dehydroepiandrosterone (DHEA), a routinely used inhibitor of G6PD, then 2 Gy irradiated. A clonogenic assay was used to measure cell survival (Fig. 5D). As before, a 2 Gy radiation exposure resulted in approximately 80% survival. Treatment with DHEA alone decreased survival to approximately 50%. However, treatment with a combination of DHEA and radiation resulted in approximately 10% survival (Fig. 5D; inset shows representative dishes with colonies). In summary, these results suggest that radioresistance of quiescent cancer cells is mediated by FOXM1-dependent G6PD expression, therefore activating the pentose phosphate pathway.

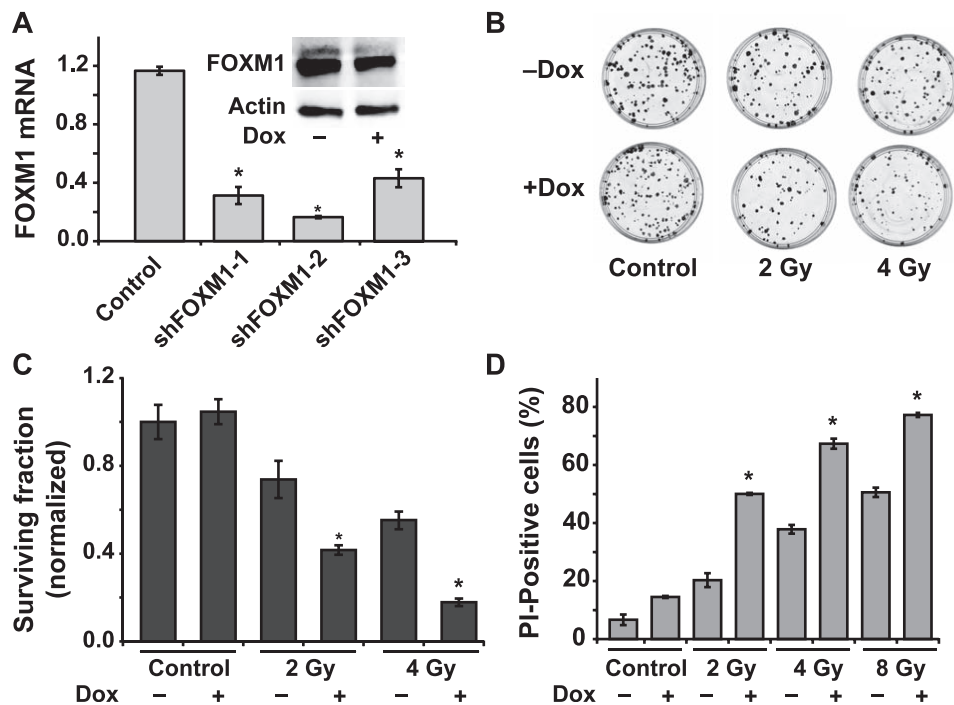


FIG. 4. Molecular knockdown of FOXM1 sensitizes quiescent HNSCC to radiation. Panel A: shFOXM1 Cal27 cells were generated and induced with doxycycline (1 μ M). mRNA of control and shFOXM1 clones 1–3 were measured using a Q-RT-PCR assay; inset: Western blot analysis of FOXM1 in shFOXM1 clone 2 with and without doxycycline (DOX) induction. Asterisks represent statistical significance of knockdown of FOXM1 mRNA compared to individual noninduced shFOXM1 Cal27 cells. $n = 3$; $P < 0.05$. Panel B: Representative dishes from a clonogenic assay showing colonies of Cal27 in wild-type and shFOXM1-2 Cal27 cells irradiated with 2 and 4 Gy. Panel C: Normalized surviving fraction was calculated relative to untreated and DOX-treated cells. Panel D: Percentage of propidium iodide (PI)-positive (nonviable) cells in shFOXM1-2 Cal27 cells with and without doxycycline-induced knockdown and 0-, 2-, 4- and 8-Gy irradiation. Asterisks represent statistical significance compared to noninduced, irradiated shFOXM1 Cal27 cells. $n = 3$; $P < 0.05$.

DISCUSSION

Quiescence-associated radioresistance may limit a successful cancer therapy outcome. Our results show that quiescent HNSCC (Cal27 and FaDu) are radioresistant. Both RNAi and pharmacological knockdown of FOXM1 expression sensitized quiescent cells to radiation treatment. Knockdown of FOXM1 was associated with a decrease in G6PD expression and inhibition of G6PD sensitized quiescent HNSCC to radiation. These results suggest that a metabolic shift regulates FOXM1-dependent radioresistance of quiescent HNSCC (Fig. 6).

Cellular quiescence is a reversible process where cells retain their capacity to re-enter the proliferative cycle after entering quiescence. Although the mechanisms regulating quiescence are not completely understood, quiescent cells are known to have a lower RNA content than proliferating cells. This is consistent with our observation of a lower RNA content in quiescent compared to proliferating HNSCC (Fig. 1A and B). We and others have shown previously that the expression of MnSOD increased significantly in quiescent cells, indicating that the cellular redox environment varies between proliferative and quiescent states (11–14). This premise is also supported by

results obtained from the Antioxidant Mechanisms PCR-array (data not shown) and Q-RT-PCR assays [Fig. 1D (Supplementary Fig. S2; <http://dx.doi.org/10.1667/RR13726.1.S1>)], suggesting that the cell growth-state specific expression of oxidative stress response genes could contribute to the difference in radiation response of proliferating and quiescent HNSCC [Fig. 1C (Supplementary Fig. S1; <http://dx.doi.org/10.1667/RR13726.1.S1>)]. Interestingly, the radiation-induced changes in the expression of oxidative stress response genes were specific to HNSCC growth state (Fig. 2A and B). A dose-dependent increase in FOXM1 expression was observed in irradiated quiescent Cal27 and FaDu cells (Fig. 2C and D), suggesting that FOXM1 could regulate radioresistance of quiescent cells.

FOXM1 is a member of the forkhead box (FOX) family of transcription factors, which play several important roles in mammalian cells, including development, differentiation, proliferation and longevity (33–35). FOX proteins are a family of evolutionarily conserved transcription factors that contain a common winged helix DNA-binding domain (34). In general, the expression of FOXO3a is upregulated during quiescence and downregulated during proliferation, while the expression of FOXM1 is downregulated in quiescent

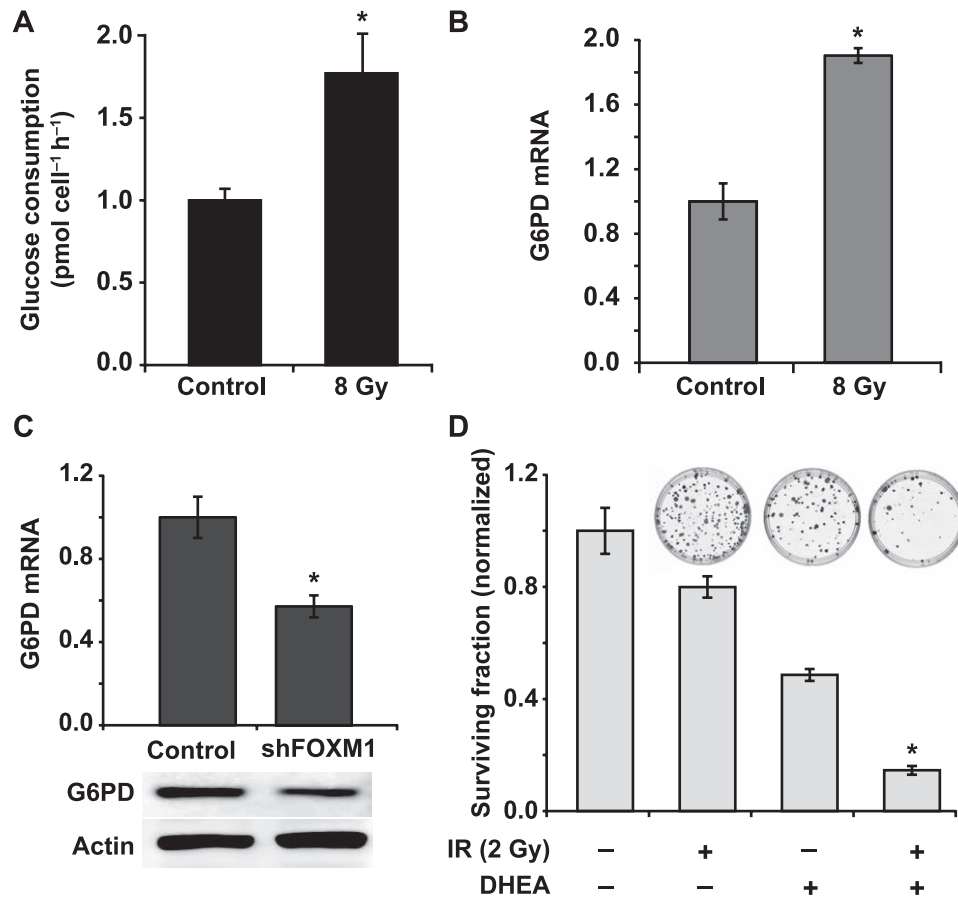


FIG. 5. Downregulation of G6PD, a downstream target of FOXO1 sensitizes quiescent HNSCC to radiation. Panel A: Glucose consumption rate in control and 8 Gy irradiated quiescent Cal27 cells was measured at 48 h postirradiation. Panel B: A Q-RT-PCR assay was used to measure G6PD mRNA expression in control and 8 Gy irradiated quiescent Cal27 cells at 48 h postirradiation. Asterisk represents statistical significance compared to unirradiated quiescent Cal27 cells. $n = 3$; $P < 0.05$. Panel C: mRNA and protein expression of G6PD in shFOXO1 Cal27 cells was measured by using a Q-RT-PCR and Western blotting assays. Asterisks indicate statistical significance compared to noninduced shFOXO1 Cal27 cells. $n = 3$; $P < 0.05$. Panel D: A clonogenic assay was used to examine surviving fraction in 2 Gy irradiated Cal27 cells pretreated with and without G6PD inhibitor, DHEA. Representative dishes of colonies are included for comparison. Asterisks represent statistical significance of combined treatment compared to radiation or DHEA treatment alone. $n = 3$; $P < 0.05$.

cells and significantly upregulated in proliferating cells (18). FOXO3a has been shown to protect quiescent cells from oxidative stress-induced toxicity by activating the expression of MnSOD (36). Although the expression of FOXO1 is significantly downregulated during quiescence (Fig. 1D), its expression increased significantly in irradiated quiescent HNSCC (Fig. 2). Additionally, pharmacological (thiostrepton) and molecular (shFOXO1) knockdown of FOXO1 expression sensitized quiescent HNSCC to radiation-induced cell death (Figs. 3 and 4). These results indicate that FOXO1 has other functions in addition to its well known pro-proliferative effects that support cell cycle progression. This study identifies FOXO1 as a previously unrecognized molecular player in regulating radioresistance of quiescent HNSCC.

Recently published data showed that FOXO1 regulates MnSOD, CAT and PRDX3 expression in IMR90 human primary fibroblasts (23). Because the expression of

MnSOD, CAT and PRDX3 is closely related to cellular metabolism, these results also suggest that FOXO1 may regulate cellular metabolism. Previous studies have shown that changes in cellular metabolic pathways influence radiation response (37, 38). Cellular metabolism in mammals consists of two main pathways: glycolysis and the pentose phosphate pathway (PPP). G6PD is the initial and rate-limiting step of the PPP. An earlier study by Tuttle *et al.* showed that G6PD-deficient Chinese hamster ovarian fibroblasts (CHO) are more sensitive to radiation-induced toxicity compared to wild-type CHO cells (31), suggesting a regulatory role of G6PD and cellular metabolism in cellular response to radiation. Consistent with this hypothesis, our results showed a higher glucose consumption rate in irradiated quiescent Cal27 cells and an increase in G6PD mRNA levels (Fig. 5A and B) correlating with an increase in FOXO1 expression (Fig. 2) and radioresistance. Interestingly, shRNA-mediated inhibition of FOXO1 ex-

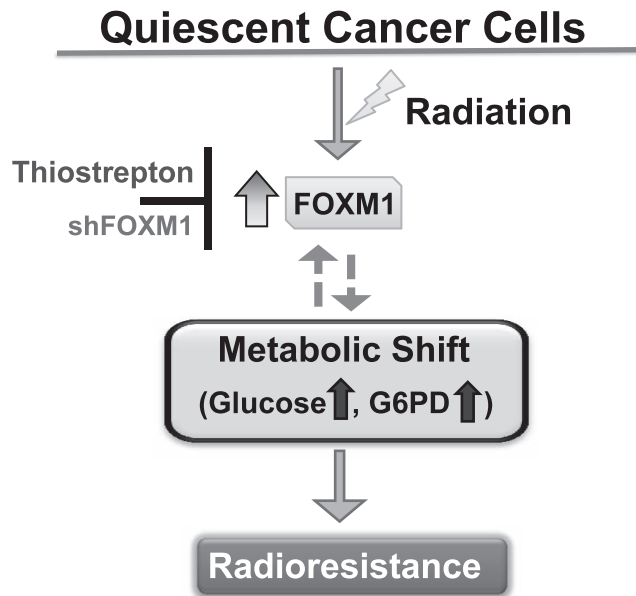


FIG. 6. A metabolic shift mediates FOXM1 regulated radioresistance of quiescent HNSCC.

pression was associated with an inhibition of G6PD expression and correlated with radiation sensitivity of quiescent HNSCC (Figs. 4 and 5C). The decrease in G6PD expression in FOXM1 knockdown Cal27 cells was also associated with approximately 15% decrease in cellular GSH content compared to wild-type cells. It is possible that the FOXM1 target sequence present in the second intron of G6PD may regulate its expression in response to radiation treatment. A role of the PPP regulating radioresistance of quiescent Cal27 cells was also evident from the results shown in Fig. 5D where pharmacological inhibition of G6PD significantly sensitized quiescent Cal27 cells to radiation-induced toxicity.

In summary, results from this study suggest that a shift in cellular metabolism mediates FOXM1-dependent radioresistance of quiescent HNSCC. Because radiation is the major treatment modality for locally advanced head and neck cancer, and approximately 40% of these patients may ultimately succumb to their disease (5), results from this study may be of great significance in developing additional cancer therapy approaches targeted at tumor cell metabolism and quiescence.

SUPPLEMENTARY INFORMATION

Table S1. PCR primers used in this study.

Fig. S1. Quiescent FaDu HNSCC cells are radioresistant. A clonogenic assay designed to accommodate post-lethal damage repair was used to examine surviving fraction in FaDu HNSCC. Asterisks represent statistical significance of quiescent compared to proliferating cells. $n = 3$; $P < 0.05$.

Fig. S2. Quiescent HNSCC have lower expression of FOXM1 than proliferating cells. Panel A: A Q-RT-PCR

assay was used to measure FOXM1 mRNA levels in proliferating and quiescent FaDu cells. Fold change in mRNA levels in quiescent cells was calculated relative to corresponding mRNA levels in proliferating cells. Asterisks represent statistical significance of quiescent compared to proliferating FaDu cells. $n = 3$; $P < 0.05$. Panel B: Western blot analysis of FOXM1 in proliferating and quiescent Cal27 and FaDu cells.

Fig. S3. Irradiated quiescent Cal27 cells do not show a difference in cell cycle phase distribution. Flow cytometry measurements of cell cycle phase distributions in quiescent Cal27 cells following radiation.

ACKNOWLEDGMENTS

We thank Dr. Netanya Spencer for G6PD antibody, Mr. Wusheng Xiao for G6PD PCR primers, Mr. Neil Patel for technical assistance, Dr. Andrean Simons for use of the glucometer, Dr. Douglas Spitz for the Cal27 and FaDu cell lines and the staff at the Flow Cytometry and Radiation and Free Radical Research Core Facilities. Funding from NIH grants 2R01 CA111365 (PCG), T32 CA078586 (JE) and T32 HL07734 (VST) supported this work.

Received: February 25, 2014; accepted: June 30, 2014; published online: September 17, 2014

REFERENCES

1. Collier HA. Cell biology. The essence of quiescence. *Science* 2011; 334:1074–5.
2. Collier HA, Sang L, Roberts JM. A new description of cellular quiescence. *PLoS Biol* 2006; 4:e83.
3. Luk CK, Keng PC, Sutherland RM. Radiation response of proliferating and quiescent subpopulations isolated from multicellular spheroids. *Br J Cancer* 1986; 54:25–32.
4. Masunaga S, Ono K. Significance of the response of quiescent cell populations within solid tumors in cancer therapy. *J Radiat Res* 2002; 43:11–25.
5. Davies L, Welch HG. Epidemiology of head and neck cancer in the United States. *Otolaryngol Head Neck Surg* 2006; 135:451–7.
6. Du C, Gao Z, Venkatesha VA, Kalen AL, Chaudhuri L, Spitz DR, et al. Mitochondrial ROS and radiation induced transformation in mouse embryonic fibroblasts. *Cancer Biol Ther* 2009; 8:1962–71.
7. Fisher CJ, Goswami PC. Mitochondria-targeted antioxidant enzyme activity regulates radioresistance in human pancreatic cancer cells. *Cancer Biol Ther* 2008; 7:1271–9.
8. Gao Z, Sarsour EH, Kalen AL, Li L, Kumar MG, Goswami PC. Late ROS accumulation and radiosensitivity in SOD1-overexpressing human glioma cells. *Free Radic Biol Med* 2008; 45:1501–9.
9. Kalen AL, Sarsour EH, Venkataraman S, Goswami PC. Mn-superoxide dismutase overexpression enhances G2 accumulation and radioresistance in human oral squamous carcinoma cells. *Antioxid Redox Signal* 2006; 8:1273–81.
10. Hutter DE, Till BG, Greene JJ. Redox state changes in density-dependent regulation of proliferation. *Exp Cell Res* 1997; 232:435–8.
11. Sarsour EH, Venkataraman S, Kalen AL, Oberley LW, Goswami PC. Manganese superoxide dismutase activity regulates transitions between quiescent and proliferative growth. *Aging Cell* 2008; 7:405–17.
12. Sarsour EH, Kalen AL, Xiao Z, Veenstra TD, Chaudhuri L, Venkataraman S, et al. Manganese superoxide dismutase regulates a metabolic switch during the mammalian cell cycle. *Cancer Res* 2012; 72:3807–16.

13. Li N, Oberley TD. Modulation of antioxidant enzymes, reactive oxygen species, and glutathione levels in manganese superoxide dismutase-overexpressing NIH/3T3 fibroblasts during the cell cycle. *J Cell Physiol* 1998; 177:148–60.
14. Oberley TD, Schultz JL, Li N, Oberley LW. Antioxidant enzyme levels as a function of growth state in cell culture. *Free Radic Biol Med* 1995; 19:53–65.
15. Tuteja G, Kaestner KH. SnapShot: forkhead transcription factors I. *Cell* 2007; 130:1160.
16. Tuteja G, Kaestner KH. Forkhead transcription factors II. *Cell* 2007; 131:192.
17. Lehmann OJ, Sowden JC, Carlsson P, Jordan T, Bhattacharya SS. Fox's in development and disease. *Trends Genet* 2003; 19:339–44.
18. Laoukili J, Stahl M, Medema RH. FoxM1: at the crossroads of ageing and cancer. *Biochim Biophys Acta* 2007; 1775:92–102.
19. Laoukili J, Kooistra MR, Bras A, Kaw J, Kerkhoven RM, Morrison A, et al. FoxM1 is required for execution of the mitotic programme and chromosome stability. *Nat Cell Biol* 2005; 7:126–36.
20. Wang IC, Chen YJ, Hughes D, Petrovic V, Major ML, Park HJ, et al. Forkhead box M1 regulates the transcriptional network of genes essential for mitotic progression and genes encoding the SCF (Skp2-Cks1) ubiquitin ligase. *Mol Cell Biol* 2005; 25:10875–94.
21. Raychaudhuri P, Park HJ. FoxM1: a master regulator of tumor metastasis. *Cancer Res* 2011; 71:4329–33.
22. Pilarsky C, Wenzig M, Specht T, Saeger HD, Grutzmann R. Identification and validation of commonly overexpressed genes in solid tumors by comparison of microarray data. *Neoplasia* 2004; 6:744–50.
23. Park HJ, Carr JR, Wang Z, Nogueira V, Hay N, Tyner AL, et al. FoxM1, a critical regulator of oxidative stress during oncogenesis. *EMBO J* 2009; 28:2908–18.
24. Kwok JM, Myatt SS, Marson CM, Coombes RC, Constantinidou D, Lam EW. Thiostrepton selectively targets breast cancer cells through inhibition of forkhead box M1 expression. *Mol Cancer Ther* 2008; 7:2022–32.
25. Bhat UG, Halasi M, Gartel AL. Thiazole antibiotics target FoxM1 and induce apoptosis in human cancer cells. *PLoS One* 2009; 4:e5592.
26. Hegde NS, Sanders DA, Rodriguez R, Balasubramanian S. The transcription factor FOXM1 is a cellular target of the natural product thiostrepton. *Nat Chem* 2011; 3:725–31.
27. Talior I, Yarkoni M, Bashan N, Eldar-Finkelman H. Increased glucose uptake promotes oxidative stress and PKC-delta activation in adipocytes of obese, insulin-resistant mice. *Am J Physiol Endocrinol Metab* 2003; 285:E295–302.
28. Vander Heiden MG, Cantley LC, Thompson CB. Understanding the Warburg effect: the metabolic requirements of cell proliferation. *Science* 2009; 324:1029–33.
29. Tuttle S, Stamato T, Perez ML, Biaglow J. Glucose-6-phosphate dehydrogenase and the oxidative pentose phosphate cycle protect cells against apoptosis induced by low doses of ionizing radiation. *Radiat Res* 2000; 153:781–7.
30. Biaglow JE, Clark EP, Epp ER, Morse-Guadio M, Varnes ME, Mitchell JB. Nonprotein thiols and the radiation response of A549 human lung carcinoma cells. *Int J Radiat Biol Relat Stud Phys Chem Med* 1983; 44:489–95.
31. Venkatesha VA, Kalen AL, Sarsour EH, Goswami PC. PCB-153 exposure coordinates cell cycle progression and cellular metabolism in human mammary epithelial cells. *Toxicology Lett* 2010; 196:110–6.
32. Myatt SS, Lam EW. Targeting FOXM1. *Nat Rev Cancer* 2008; 8:242.
33. Myatt SS, Lam EW. The emerging roles of forkhead box (Fox) proteins in cancer. *Nat Rev Cancer* 2007; 7:847–59.
34. Arden KC. Multiple roles of FOXO transcription factors in mammalian cells point to multiple roles in cancer. *Exp Gerontol* 2006; 41:709–17.
35. Kops GJ, Dansen TB, Polderman PE, Saarloos I, Wirtz KW, Coffey PJ, et al. Forkhead transcription factor FOXO3a protects quiescent cells from oxidative stress. *Nature* 2002; 419:316–21.
36. Spitz DR, Azzam EI, Li JJ, Gius D. Metabolic oxidation/reduction reactions and cellular responses to ionizing radiation: a unifying concept in stress response biology. *Cancer Metastasis Rev* 2004; 23:311–22.
37. Azzam EI, Jay-Gerin JP, Pain D. Ionizing radiation-induced metabolic oxidative stress and prolonged cell injury. *Cancer Lett* 2012; 327:48–60.
38. Eckers JK, AL; Xiao, W; Sarsour, EH; Goswami, PC. Selenoprotein P inhibits radiation-induced late reactive oxygen species accumulation and normal cell injury. *Int J Radiat Oncol Biol Phys* 2013; 87:619–25.